Glycobiology Advance Access published August 24, 2015

Structural determinants of heparin-transforming growth factor-β1 interactions and their effects on signalling

Jonathan Lee[1,2], Sheena Wee[3], Jayantha Gunaratne[3], R. J. E. Chua[2], Raymond A. A. Smith[2], Ling Ling[2], David G. Fernig[4], Kunchithapadam Swaminathan[5], Victor Nurcombe[2,6,*] and Simon M. Cool[2,7,*]

[1]NUS Graduate School for Integrative Sciences and Engineering, National University of Singapore, Singapore 117456

[2]Glycotherapeutics Group, Institute of Medical Biology, Agency for Science, Technology and Research, Singapore 138648

[3]Quantitative Proteomics Group, Institute of Molecular and Cell Biology, Agency for Science, Technology and Research, Singapore 138673

[4]Department of Biochemistry, Institute of Integrative Biology, University of Liverpool, Liverpool L69 7ZB, United Kingdom

[5]Department of Biological Sciences, National University of Singapore, Singapore 117543

[6]Lee Kong Chian School of Medicine, Nanyang Technological University-Imperial College, Singapore 639798

[7]Department of Orthopaedic Surgery, Yong Loo Lin School of Medicine, National University of Singapore, Singapore 119228

Corresponding authors: Dr. Simon M. Cool, Tel: (65) 6407 0176, Fax: (65) 6478 9477, E-mail: simon.cool@imb.a-star.edu.sg, Dr. Victor Nurcombe, Tel: (65) 6407 0176, Fax: (65) 6478 9477, E-mail: victor.nurcombe@imb.a-star.edu.sg

© The Author 2015. Published by Oxford University Press. All rights reserved. For permissions, please e-mail: journals.permissions@oup.com

Downloaded from http://glycob.oxfordjournals.org/ at UniversitÃ¤tsbibliothek OsnabrÃ¼ck on January 12, 2016

Abstract

Transforming growth factor-β1 (TGF-β1, Uniprot: P01137) is a heparin-binding protein that has been implicated in a number of physiological processes, including the initiation of chondrogenesis by human mesenchymal stem cells (hMSCs). Here we identify the molecular features in the protein and in heparin required for binding and their effects on the potentiation of TGF-β1's activity on hMSCs. Using a proteomics "Protect and Label" approach, lysines K291, K304, K309, K315, K338, K373, K375 and K388 were identified as being directly involved in binding heparin. Competition assays in an optical biosensor demonstrated that TGF-β1 does require *N*- and 6-*O*-sulphate groups for binding, but that 2-*O*-sulphate groups are unlikely to underpin the interaction. Heparin-derived oligosaccharides as short as degree of polymerisation (dp) 4 have a weak ability to compete for TGF-β1 binding to heparin, which increases with the length of the oligosaccharide to reach a maximum between dp18 and dp24. In cell-based assays heparin, 2-*O*-, 6-*O*- and *N*-desulphated re-*N*-acetylated heparin, and oligosaccharides 14-24 saccharides (dp14-24) in length all increased the phosphorylation of SMAD2 after 6 h stimulation with TGF-β1. The results provide the structural basis for a model of heparin/HS binding to TGF-β1 and demonstrate that features in the polysaccharide required for binding are not identical to those required for sustaining the signalling by TGF-β1 in hMSCs.

Keywords: Heparan sulphate/Heparin/Proteoglycans/Transforming growth factor-β1

Downloaded from http://glycob.oxfordjournals.org/ at UniversitÃ¤tsbibliothek OsnabrÃ¼ck on January 12, 2016

Introduction

The glycosaminoglycans (GAGs) heparan sulphate (HS) and heparin are structurally closely related linear polysaccharides that are known to bind numerous extracellular proteins and growth factors and modulate their functions (Ori, et al. 2011). Transforming growth factor-β1 (TGF-β1, Uniprot: P01137) is a potent heparin-binding growth factor (Lyon, et al. 1997, McCaffrey, et al. 1989, McCaffrey, et al. 1992, McCaffrey, et al. 1994) that has been shown to play roles in fibrosis (Lee, et al. 2011, Watson, et al. 2010), skin healing (Siebert, et al. 2011), cancer metastasis (Jakowlew 2006, Yang, et al. 2002) and chondrogenesis (Grimaud, et al. 2002, Rosen, et al. 1997, Toh, et al. 2005, van der Kraan, et al. 2009, Yang, et al. 2001). This ability of TGF-β1 to drive the chondrogenic differentiation of human mesenchymal stem cells (hMSCs) and maintain the chondrogenic phenotype has made it of particular interest for the development of cartilage repair strategies (Sato, et al. 2007, Toh, et al. 2005, Wang, et al. 2010, Wang, et al. 2014).

Like many other members of its family, TGF-β1 has been shown to be a heparin-binding protein (McCaffrey, et al. 1989, McCaffrey, et al. 1992, McCaffrey, et al. 1994) and a model for its interaction with this GAG has been proposed (Lyon, et al. 1997), but to date no direct measurement or determination of the interacting chemical groups has been reported. Similarly, there are data on sulphation patterns in the polysaccharide required for potentiating the activity of TGF-β1 in cultured cells (Lyon, et al. 1997), but no data pertaining to the actual interaction of the protein with the GAG. Thus, there is a fundamental need to determine the structural basis for the interaction of TGF-β1 with heparin from the perspective of both the protein and the GAG.

Using a structural proteomics approach, previously dubbed “Protect and Label” (Ori, et al. 2009), we identify the lysine residues in TGF-β1 that are involved in its binding to heparin. Subsequently, the effects of heparin chain length and sulphation pattern on TGF-β1 binding and bioactivity were determined with an optical biosensor (Biacore) competition assay. By measuring the effect of heparin and its derivatives on SMAD phosphorylation in hMSCs, we show that the structural features that determine TGF-β1’s interaction with the polysaccharide do not predict whether it can prolong the activity of TGF-β1. These data are used to develop a model for the interaction of TGF-β1 and heparin/HS, and a basis for variation in heparin binding across the TGF-β superfamily.

Downloaded from http://glycob.oxfordjournals.org/ at UniversitÃ¤tsbibliothek OsnabrÃ¼ck on January 12, 2016

Results

Heparin binds to TGF-β1

To explore the structural requirements and constraints inherent to the heparin-TGF-β1 interaction, the ability of TGF-β1 to bind to heparin was first validated. To do so, heparin biotinylated on internal free amine groups was immobilised on a streptavidin sensor surface (~40 RUs) and TGF-β1 samples (50 – 800 nM) injected over this to determine binding (Fig. 1A). TGF-β1 was observed to bind to the heparin-derivatised surface in a dose-dependent manner, but K_d, k_{on} and k_{off} values could not be determined, as the data did not fit a 1:1 binding model. The binding was confirmed using GAG-binding plates onto which heparin was absorbed and bound TGF-β1 detected via ELISA. Again, TGF-β1 was observed to bind to heparin in a dose-dependent manner (Fig. 1B).

Identification of heparin-binding sites within TGF-β1

We next sought to identify the residues in TGF-β1 that were involved in this interaction. Previous studies that sought to identify putative heparin-binding sites on TGF-β1 did so through either the identification of contiguous heparin-binding motifs present in the protein sequence (McCaffrey, et al. 1992), or through differences in basic residues between the sequences of heparin-binding and non-binding TGF-β isoforms (Lyon, et al. 1997). However, the former approach is unable to identify heparin-binding sites that consist of amino acids brought into proximity by protein folding (Ori, et al. 2008), while the later cannot determine if the identified residues are truly part of a heparin-binding site. We therefore used the "Protect and Label" approach developed by Ori et al. (2009) to identify directly those lysine residues most likely to be involved in the binding of TGF-β1 and heparin. Briefly, the technique involves the selective labelling of solvent-exposed lysine residues in a given heparin-protein complex, using *N*-hydroxysuccinimide (NHS)-based chemistry (Fig. 2A). This selective labelling enables the identification of lysines that directly interact with heparin, and their location in the protein, through tandem mass spectrometry (MS/MS) sequencing. Additionally, this technique is unlikely to identify non-specific electrostatic interactions between the target protein and heparin, because of the duration of the protection/acetylation step (5 min). Over this time, such interactions will dissociate, since they are characterised by very fast kinetics. Thus, the lysines involved in such non-specific ionic interactions will be protected and not subsequently labelled/biotinylated and so

Downloaded from http://glycob.oxfordjournals.org/ at UniversitÃ¤tsbibliothek OsnabrÃ¼ck on January 12, 2016

identified as a heparin-binding residue (Ori et al., 2009). In fact, previous reports have shown that even in canonical heparin-binding sites, there is partial acetylation of some lysine residues, due to the local dissociation of these interactions over the duration of the protection/acetylation step (Uniewicz, et al. 2014, Xu, et al. 2012). During the selective labelling process, samples of the TGF-β1 were taken at several points along the experimental pipeline, resolved by denaturing SDS-PAGE and silver stained (Fig. 2B), to determine that significant amounts of protein were not being lost at any stage. As all samples were expected to run as ~12.5 kDa monomers after denaturation in Laemmli buffer, the 25 kDa dimer observed in lane 1 was unexpected. These may be artefactual dimers resulting from the high concentration of protein (~1 μg) collected for the sample (Hames 1998).

In the case of TGF-β1, the protein remained bound to heparin during the first column wash (Fig. 2B, sample 2). A small amount of protein was recovered after the protection/acetylation step (Sample 3), which indicated that the interaction between TGF-β1 and heparin may be dynamic to some extent at the level of individual atomic interactions. In such an instance, the transient exposure of a heparin-binding lysine to the solvent would have led to the acetylation of the residue and so prevent it from re-binding the polysaccharide. This could lead to further lysines dissociating transiently and the protein dissociating from the column, as observed here. In contrast to TGF-β1 bound to heparin agarose (Lyon, et al. 1997) 2 M NaCl was unable to effectively elute the acetylated TGF-β1 from the Toyopearl AF-Heparin affinity column, so RapiGest, an acid-labile detergent, was employed instead (Sample 4) (Fig. S1). The subsequent concentration, labelling/biotinylation and de-salting of the TGF-β1 sample (Fig. 2B, lanes 5, 6 and 7) led to minor loss of sample, but sufficient amounts were recovered for chymotryptic digest, Strep-Tactin purification and MS/MS.

Thirty-one ions were generated and assigned to 11 representative peptides, which cover all the acetylation and biotinylation sites in the sequence of TGF-β1 (Table 1). Two peptides did not contain any biotinylated lysines, which was unexpected, as peptides were purified on Strep-Tactin-Sepharose. Whilst these peptides may have bound non-specifically to the Strep-Tactin-Sepharose, the fact that the same peptides with biotinylated lysines were also identified (Tables S1 and 1) indicates that these do indeed correspond to part of the heparin-binding site of TGF-β1. Two pairs of peptides (Table S1, ions 1, 5, 12 and 4, 6, 21, and ions 10, 16, 20, 29, 31 and 10, 11, 18-20, 29, 30; Table 1 peptides 4 and 5, and 8 and 9) were found to contain lysines that were observed to be biotinylated or acetylated, which supports the argument that the heparin-TGF-β1 interaction is dynamic at the atomic level,

Downloaded from http://glycob.oxfordjournals.org/ at UniversitÃ¤tsbibliothek OsnabrÃ¼ck on January 12, 2016

with individual lysines dissociating and re-binding in the time of the protection step. Finally, the MS/MS spectra for peptide 7 (Table S1, ion 8) contained unassigned peaks, so there is a possibility, although minor, that its actual sequence may differ from the one listed in Table 1.

When mapped onto the full amino acid sequence of TGF-β1, five lysines that had been predicted to be involved in heparin binding were identified, K304, K309, K315, K373 and K375 (Fig. 3A) (Lyon, et al. 1997, McCaffrey, et al. 1992). A further three lysines, K291, K338 and K388 were also found to be protected by heparin and so biotinylated. K338 has been postulated to be part of a secondary heparin-binding site in TGF-β1 (Lyon, et al. 1997), whereas K291 and K388 have not been associated with heparin binding previously. When these lysines are mapped onto the 3-dimensional solution structure of TGF-β1 (PDB: 1KLC) (Hinck, et al. 1996), K291 was found to be located on the same surface of the TGF-β1 homodimer as K304 (Fig. 3B). However, the side chain of K388 appears likely to be involved in interactions with neighbouring side chains, e.g., D55, Q81 and S112, and so may not to be solvent accessible. Thus, its identification here may be due to TGF-β1 undergoing a conformational change upon heparin binding, which would expose this side chain, or an artefact of partial unfolding of the protein that may be consequent on the exposure of the protected TGF-β1 to RapiGest prior to labelling with NHS-biotin. Arginine residues and amides (as side chains or main chain) can also be involved in general heparin–protein binding (Gandrille, et al. 1990, Ori, et al. 2008). Indeed, the arginine guanidino groups will bind to sulphate more tightly than the primary amine of lysines (Fromm, et al. 1995). However, the nature of the NHS-based chemistry used precludes their labelling and identification. Importantly, our results show that arginines tend to cluster with lysines within the TGF-β1 protein sequence, so their role in binding heparin can be inferred from the data here.

Heparin length requirements for TGF-β1 binding

We next sought to determine the minimum length of heparin chain required to bind TGF-β1. The ability of soluble, size-fractionated (dp4 to dp24) heparin fragments to competitively inhibit the binding of TGF-β1 to a heparin-derivatised streptavidin sensor surface increased in proportion to their length (Fig. 4). Thus, dp4 (5 µg, 41.7 µg/mL and 10 µg, 83.3 µg/mL) reduced binding by around 20% and 40%, respectively, whereas for a length of dp18, binding was reduced by 90%, which was a little less than observed with native heparin (100%, Fig. 4).

Downloaded from http://glycob.oxfordjournals.org/ at UniversitÃ¤tsbibliothek OsnabrÃ¼ck on January 12, 2016

Heparin sulphation requirements for TGF-β1 binding

The influence that the various sulphate moieties in heparin have over the interaction with TGF-β1 was then determined. In optical biosensor (Biacore) competition assays, 2-*O*-desulphated heparin (2-*O*-de) (~95% reduction in 2-*O*-sulphates) competed nearly as efficiently as heparin for TGF-β1 binding, whereas 6-*O*-desulphated heparin (6-*O*-de) (~90% reduction in 6-*O*-sulphates and 25% loss of 2-*O*-sulphates) was a less effective competitor (Fig. 5). In contrast, *N*-desulphated re-*N*-acetylated heparin (*N*-de) (~92% reduction in *N*-sulphates) was the least effective competitor for binding of TGF-β1 to the immobilised heparin on the sensor surface. Thus, the results show that *N*- and 6-*O*-sulphate groups are likely to play a central role in binding TGF-β1 and that 2-*O*-sulphate groups have a lesser or even negligible a role.

Effects of heparin on TGF-β1 signalling in hMSCs

We next examined if the structural features identified for the interaction between heparin and TGF-β1 were the same as those influencing the cellular response to TGF-β1 signalling in hMSCs. This was measured by the downstream phosphorylation of SMAD2 and SMAD3. Heparin has been shown to potentiate the effects of TGF-β1 in primary rat and bovine smooth muscle cells (SMCs) and the CCL64 mink lung epithelial cell line, but not in primary human saphenous vein SMCs (McCaffrey, et al. 1989, McCaffrey, et al. 1994), by virtue of its protecting the protein from binding to α2-macroglobulin (Lyon et al 1997) or its enhancement of the protein's binding to cells (McCaffrey, et al. 1989). Therefore, should heparin potentiate exogenous TGF-β1 activity in hMSCs, the effects would only be seen as the phospho-SMAD2 (pSMAD2) and phospho-SMAD3 (pSMAD3) signals from TGF-β1 alone started to subside. Thus the time points chosen for our initial TGF-β1 dosing experiment were generally 6, 12, 24 and 48 h. Since hMSCs are primary human cells, there is far more variation than with primary cells from a laboratory rodent. Therefore, to provide insight into this variation, the quantification of Western blotting is reported as the actual fold-stimulation for each experiment, rather than a mean, which would to an extent mask the true variation that can be expected from these measurements (Figs. S2-5).

Downloaded from http://glycob.oxfordjournals.org/ at UniversitÃ¤tsbibliothek OsnabrÃ¼ck on January 12, 2016

Passage 5 cells were treated with a range of TGF-β1 doses in the presence of serum and total cell lysate collected between 6 h - 48 h after addition of the growth factor. Lysate samples were then resolved by SDS-PAGE and probed for pSMAD2, pSMAD3, total SMAD2/3 and actin by Western blot. Our results showed that in the absence of TGF-β1 (Fig. 6), there was a low background level of pSMAD2 and pSMAD3, but when 1 ng/mL TGF-β1 was added, the phosphorylation of SMAD2 was quite intense at 6 h and subsided to background levels at 12 h and 24 h. The phosphorylation of SMAD3 was barely detectable with 1 ng/mL TGF-β1. With 5 ng/mL TGF-β1, the phosphorylation of SMAD2 was high up to 24 h and then reduced partly by 48h, whereas at 10 ng/mL TGF-β1 the phosphorylation of SMAD2 remained at maximal levels throughout the time course. SMAD3 phosphorylation was clearly stimulated by both 5 ng/mL and 10 ng/mL TGF-β1, reaching maximal levels at 6h -12 h and then returning to basal levels by 24 h. The 6 h time point was thus chosen for all subsequent experiments.

We then determined the dose of heparin to use for our experiments. McCaffrey *et al.* (1989) have previously reported the effective TGF-β1-potentiating dose of heparin to be between 1-100 μg/mL, we chose to use doses within this range. Cells that were treated with 1 ng/mL of TGF-β1 pre-incubated with 10 μg/mL of heparin maintained a stronger pSMAD2 and pSMAD3 signal compared to cells treated with the same dose of TGF-β1 alone (Fig. 7, S2). A higher dose of heparin (40 μg/mL) with TGF-β1 was unable to elicit an effect greater than that seen for 10 μg/mL of heparin when pre-incubated with 1 ng/mL of TGF-β1. When pre-incubated with 5 ng/mL of TGF-β1, neither dose of heparin was able enhance the phosphorylation of SMAD2 and 3 beyond that obtained from the growth factor alone. Taken together, our results demonstrate that heparin prolongs rather than enhances the pSMAD signals produced by TGF-β1, which is consistent with previous reports that heparin protects TGF-β1 from inactivation through, for example, binding α2 macroglobulin (Lyon, et al. 1997, McCaffrey, et al. 1989, McCaffrey, et al. 1994).

To determine if the effect of heparin on TGF-β1 stimulation of SMAD2 and 3 phosphorylation was to prolong the activity of the growth factor, rather than enhance the assembly of a ligand-receptor signalling complex, cells were treated with heparinase I, II and III (1.2 mIU/mL each) for 24 h in hMSC culture medium, before being stimulated with TGF-β1 in serum-free medium. Serum-free medium was used to avoid the confounding effects of (i) stimulation of SMAD2 and 3 phosphorylation by the addition of fresh serum after

Downloaded from http://glycob.oxfordjournals.org/ at UniversitÃ¤tsbibliothek OsnabrÃ¼ck on January 12, 2016

heparinase treatment, and (ii) serum components, such as α2-macroglobulin, that are thought to inactivate the growth factor (Lyon, et al. 1997, McCaffrey, et al. 1989, McCaffrey, et al. 1994). Immunofluorescence staining of cell surface HS with the anti-HS 10E4 antibody showed that after 24 h treatment, nearly all the cell surface HS had been removed (Fig. 8A, B). In the absence of serum and heparinase treatment, heparin was observed to potentiate the phosphorylation of SMAD2 and 3 with 1 ng/mL TGF-β1, though with 5 ng/ml TGF-β1 the level of phosphorylation of SMAD2 and 3 was already maximal so no effect was discernable (Fig. 8C). When heparin was added to the heparinase-treated cells in serum-free medium, only a potentiation of the phosphorylation of SMAD2 by 1 ng/mL TGF-β1 was observed (Fig. 8D). These data suggest that the mechanism whereby heparin prolongs the activity of TGF-β1 in hMSCs, involves more than the prevention of its inactivation through binding to α2 macroglobulin, and that the phosphorylation of SMAD2 and 3 is differently sensitive to heparinase treatment, since only SMAD2 phosphorylation is enhanced by the addition of heparin. (Fig. 8C, D, S3). Thus, this is only partly consistent with the view that heparin protects TGF-β1 from inactivation by serum components. The data indicate that the polysaccharide may also influence endogenous cellular inhibitors and/or the assembly of signalling complexes that sustain the phosphorylation of SMAD2 and 3.

Effects of heparin length and sulphation on TGF-β1 signalling in hMSCs

We next determined whether the same structural features in the polysaccharide that promote binding of TGF-β1 also enable the TGF-β1-stimulated phosphorylation of SMAD2 and 3 to be prolonged. Western blot analysis of pSMAD2 and pSMAD3 levels in cells treated with the longer heparin-derived oligosaccharides (dp14-dp24, 10 μg/mL) and TGF-β1 (1 ng/mL) at 6 h post treatment showed similar levels of phosphorylation of these proteins as with native heparin (Fig. 9A), though there appears to be a preference for longer oligosaccharides (Fig. S4). When 2-*O*-desulphated, 6-*O*-desulphated and *N*-desulphated re-*N*-acetylated heparin were added to cells with 1 ng/mL TGF-β1, the phosphorylation of SMAD2 and 3 was increased to at least the level observed with heparin (Figs. 9B and S5). On its own, *N*-desulphated re-*N*-acetylated heparin did not have any significant effect on the levels of phosphorylated SMAD2 and SMAD3 in hMSCs when used at concentrations between 10 ng/mL-10 μg/mL. Surprisingly, despite its reduced ability to bind TGF-β1 in the optical biosensor experiments, *N*-desulphated re-*N*-acetylated heparin, like heparin, was able

Downloaded from http://glycob.oxfordjournals.org/ at UniversitÃ¤tsbibliothek OsnabrÃ¼ck on January 12, 2016

to potentiate the phosphorylation of SMAD2 and 3 by TGF-β1 (Fig. S6). The data indicate that the prolongation of the phosphorylation of SMAD2 and 3 by heparin depends only in part on the sulphation pattern of the polysaccharide, much like how the interaction of TGF-β1 with heparin is determined by more than just charge distribution.

Discussion

The interaction of TGF-β1 with heparin and HS in cultured cells potentiates its activity (Lyon, et al. 1997, McCaffrey, et al. 1989, McCaffrey, et al. 1994) and HS with appropriate structures may do the same *in vivo*. While Lyon et al. (1997) have studied the biological activity of specifically desulphated heparins with TGF-β1, there is no direct evidence for the heparin-binding site in TGF-β1 or whether sulphation patterns required for TGF-β1 binding correlate with those required for promotion of its activity. The present data demonstrate that while heparin-derived oligosaccharides as short as dp4 may interact weakly with TGF-β1, the most effective binding is achieved with dp18-dp20. A clear hierarchy exists with respect to sulphate groups with *N*- and 6-*O*- sulphates clearly required for TGF-β1 binding and *2*-*O*-sulphates playing at most a minor role.

Previous approaches to the identification of heparin-binding domains in proteins relied heavily on the identification of linear consensus sequences (Baird, et al. 1988, Cardin and Weintraub 1989, Gandhi and Mancera 2012, McCaffrey, et al. 1992). However, such an approach fails to account for the presence of binding sites that are created in the folded protein (Xu, et al. 2012). Using a technique developed by Ori *et al.* (2009), we were able to validate both the previously predicted heparin-binding sites on TGF-β1 (McCaffrey, et al. 1992) and the currently proposed binding model (Lyon, et al. 1997) (Fig. 10A). In fact, the identification here of the K291 residue improves the original model and provides a basis for the orientation of the heparin chain between the two TGF-β1 monomers (Fig. 10B). The location of the K291 residues on the protein homodimer may aid in guiding the heparin chain through the hydrophobic region that exists between the K304 residues (K26 on the Lyon *et al.* model) on either monomer. When coupled with our data on the size requirements for heparin and the report on heparin structures by Khan *et al.* (2010), it is now evident how a dp20 or dp22 would be able to bridge the distance between the opposing K304 residues. Such a bipartite heparin-binding site has also been observed in both dimeric proteins like vascular endothelial growth factor-165 (Fairbrother, et al. 1998, Soker, et al. 1994) and monomeric

Downloaded from http://glycob.oxfordjournals.org/ at UniversitÃ¤tsbibliothek OsnabrÃ¼ck on January 12, 2016

proteins like interferon-γ (Lortat-Jacob, et al. 2002, Vivès, et al. 2004). In both cases, the protein engages a heparin/HS chain through both heparin-binding sites, similar to TGF-β1.

Additionally, our data suggest that TGF-β1 may possess a secondary heparin-binding site located on the face opposite the canonical primary binding site, as postulated by Lyon et al. (1997) (Fig. 3). This is similar to the growing number of proteins that have had secondary heparin-binding sites identified, like collagen I (San Antonio, et al. 1994, Sweeney, et al. 1998), fibronectin (Lin, et al. 2000) and FGFs (Baird, et al. 1988, Ori, et al. 2009, Xu, et al. 2012). However, it is likely that this secondary binding site may only be relevant when TGF-β1 is in its active/mature form as the site is masked in the latent form. Site-directed mutagenesis of these residues would allow a more thorough assessment of this relationship.

While it is widely accepted that heparin is able to bind to TGF-β1, reports on the effects of this interaction remain conflicting. Some groups have reported that heparin potentiates TGF-β1 activity by preventing its association with, and clearance by α_2-macroglobulin (McCaffrey, et al. 1989, McCaffrey, et al. 1994), and that this effect is not seen when cells are cultured without serum (Lyon, et al. 1997). Others have reported that heparin binding to TGF-β1 has either no effect on the phosphorylation of SMAD (Yue, et al. 2008), based on a single 30 min time point, or inhibits TGF-β-SMAD signalling (Lee, et al. 2011, Mu, et al. 2012).

The measurement of the stimulation of the phosphorylation of SMAD2 and 3 by TGF-β1 in hMSCs indicates that heparin potentiates TGF-β1 signalling in these cells by increasing the half-life of the TGF-β1-driven pSMAD signal, rather than its maximum intensity. This is consistent with the previous view that the mechanism involves the protection of TGF-β1 from inactivation (Lyon, et al. 1997, McCaffrey, et al. 1989). However, the measurement of TGF-β1-stimualted SMAD2 and 3 phosphorylation in heparinase-treated and serum-starved cells is only partly consistent with this view (Figs. 8C, D), which suggests that other mechanisms may also be involved. The dependence (in the presence of serum) of the potentiation of SMAD2 and 3 phosphorylation on the structure of heparin only partly recapitulates the requirements for TGF-β1 binding. For example, whereas *N*-sulphate groups are likely to play a significant role in binding TGF-β1, the removal of *N*-sulphate does not abrogate the potentiation of TGF-β1–stimulated SMAD2 and 3 phosphorylation by heparin. Taken together with the experiments in serum-free medium, there would appear to be both endogenous cell proteins and serum proteins that can inactivate TGF-β1. Additionally, the

Downloaded from http://glycob.oxfordjournals.org/ at UniversitÃ¤tsbibliothek OsnabrÃ¼ck on January 12, 2016

potentiating effects of heparin and its derivatives would appear to be mediated by the polysaccharide binding more than just TGF-β1, because *N*-desulphated re-*N*-acetylated heparin is effective. Whether the potentiating effect requires engagement by the polysaccharide of both TGF-β1 and its inhibitors or only an interaction of heparin with the latter remains to be determined. Given the pleiotropic effects of TGF-β1, it is possible that these observations are cell-type dependent. A previous study (Lyon, et al. 1997) reported a loss of biological activity with less sulphated forms of HS in NRK 49F cells (normal rat kidney fibroblasts) after 7 days in culture relative to highly sulphated HS. This contrasts with our data on the ability of *N*-desulphated re-*N*-acetylated heparin to maintain biological activity. The measurement of phosphorylation of SMAD2 and 3 as a readout over 6 h in human MSCs may account for the observed difference. It remains to be determined if the sustained phosphorylation of SMAD2 and 3 lead to significant changes in gene expression and cellular behaviour.

The observation that long oligosaccharides (dp18-dp22) bind TGF-β1 most effectively suggests that the number of HS structures that TGF-β1 recognises in the extracellular matrix (ECM) would be substantially less than those recognised by FGF-2, for example, which only requires a dp4 (Delehedde, et al. 2002). Such long sulphated structures will be rare in most cellular HS (Murphy, et al. 2004). It may be that TGF-β1 can bind effectively across S-transition-acetylated-transition-S (NS/NA) domain units of this length, which would be more common in HS, as found for some chemokines (Lortat-Jacob, et al. 2002). However, such units may also be less likely to be fully free of endogenous heparin-binding proteins, since there are many of these (Ori, et al. 2011). Therefore, the implications for the subsequent transport of mature TGF-β1 in the ECM, like that of FGF2, is likely to be controlled by the affinity and number of HS binding sites (Duchesne, et al. 2012). TGF-β1 would consequently diffuse more quickly and further away from its site of production. As TGF-β1 is also known to be a potent chemotactic factor (Wahl, et al. 1987), this may be an evolutionary mechanism for the differential regulation of chemokines and cytokines, where the former generally need to act at greater distances than the latter.

The data imply that TGF-β1-binding sites in HS, which require a long sequence of saccharides, *N*- and 6-*O*-sulphation are more likely to span an S-domain and its flanking NS/NA transition domains or even two such units and the intervening NA domain. The presence of N-acetyl glucosamine in such structures increases the flexibility of the glycosidic bond, since there is no transient H-bonding possible to the adjacent uronic acid (Yates, et al.

Downloaded from http://glycob.oxfordjournals.org/ at UniversitÃ¤tsbibliothek OsnabrÃ¼ck on January 12, 2016

1996). Thus our proposed model for TGF-β1-heparin binding (Fig. 10B), where the greater degree of flexibility and lower (absent for NA domain) sulphation of the central unit of the HS chain allows it to bridge the hydrophobic space between the identified heparin-binding sites on either end of the TGF-β1 dimer.

TGF-β1 has been shown to play roles in fibrosis (Lee, et al. 2011, Watson, et al. 2010), skin healing (Siebert, et al. 2011), cancer metastasis (Jakowlew 2006, Yang, et al. 2002) and chondrogenesis (Grimaud, et al. 2002, Rosen, et al. 1997, Toh, et al. 2005, van der Kraan, et al. 2009, Yang, et al. 2001). Its activity is very tightly regulated through its production in a latent form, known as latent TGF-β (LTGF), and the subsequent binding of LTGF to LTGF binding proteins (LTBPs), which in turn are sequestered in the ECM. Activation of latent TGF-β1 (LTGF) has been reported to be inhibited by heparin, through the binding of the heparin chain to both the mature TGF-β1 protein and the latency associated peptide (LAP) (Lee 2013). The crystal structure of porcine LTGF shows that the LAP wraps around the mature TGF-β homodimer like a pincer (PDB: 3RJR) (Shi, et al. 2011) (Fig. 10C) and disrupts the structure of the heparin-binding site (Fig. 10D). It is possible that a heparin/HS chain could bind LTGF and secure the mature TGF-β1 within the grasp of LAP, as suggested by Lee (Lee 2013) (Fig. 10E), or that a heparin/HS chain could bind to mature TGF-β1 and prevent its association with LAP (Fig. 10D). These hypotheses are not currently distinguishable and may explain the conflicting reports on the effect of heparin on TGF-β1 activity, since the effects seen are cell and tissue-dependent, because the function of both TGF-β1 and HS varies with tissue type (Bramono, et al. 2012, Manton, et al. 2006, Murali, et al. 2011, Murali, et al. 2009, Nurcombe, et al. 2007). However, it is clear that the postulated secondary heparin-binding site in TGF-β1 is clearly masked by LAP in LTGF. For hMSCs, heparin appears to act in the latter role, where the GAG chain prevents LAP from associating with mature TGF-β1, as the results here indicate that active levels of TGF-β1 are maintained for longer periods, based on the increased duration of SMAD phosphorylation.

The work reported here provides the structural basis for a model of heparin/HS binding to TGF-β1 and demonstrates that features in the polysaccharide required for binding are not identical to those required for sustaining the signaling by TGF-β1 in hMSCs.

Downloaded from http://glycob.oxfordjournals.org/ at UniversitÃ¤tsbibliothek OsnabrÃ¼ck on January 12, 2016

Materials and methods

Surface plasmon resonance (SPR)

Internally biotinylated heparin was prepared based on the protocol reported by Hernaiz et al. (2000). Briefly, 20 mg of heparin was filter-sterilised (0.22 μm) in 1 mL of water and incubated with 8.6 μmol of *N*-hydroxysuccinimide-biotin (NHS-biotin) (Thermo Fisher Scientific, MA, USA) in 20 μL of dimethyl sulfoxide (DMSO) for 2 h at 4°C. The biotinylated heparin was then extensively dialysed (7000 MWCO) to remove unreacted biotin. Immobilisation of the biotinylated heparin onto a streptavidin (SA) sensor surface (GE Healthcare, Uppsala, Sweden) was carried out using the in-built immobilisation protocol on the Biacore T100 (GE Healthcare, Uppsala, Sweden) with a targeted immobilisation level of approximately 40 response units (RUs), where 1 RU is equivalent to ~1 pg of protein/mm^2 although the equivalent value for heparin has never been determined. HBS-EP running buffer (10 mM HEPES, 150 mM NaCl, 3.0 mM EDTA, 0.05% (v/v) Tween 20, pH 7.4) was used for the immobilisation.

TGF-β1-heparin interactions were effected by preparing a series of TGF-β1 protein samples, 50 to 800 nM final concentrations, diluted in HBS-EP-0.1 running buffer (0.1% instead of 0.05% (v/v) Tween 20). The sample solutions were then injected over the heparin-coated surface at a flow rate of 30 μL/min for 120 s, with HBS-EP-0.1 being subsequently passed over the surface for a further 600 s to monitor TGF-β1 dissociation. After dissociation, the sensor surface on the chip was regenerated by 2 washes of 2 M NaCl injected at 30 μL/min for 60 s. In control experiments, the binding of 200 nM TGF-β1 to the uncoated streptavidin surface was ~40 RUs, while binding to the heparin-derivatised surface was ~140 RUs.

Competitive binding experiments were carried out as above, with a final concentration of 200 nM TGF-β1 in HBS-EP-0.1 mixed with either 5 or 10 μg (41.7 or 83.3 μg/mL, respectively) of heparin (Sigma-Aldrich, MO, USA) or heparin derivative (Iduron Ltd, Manchester, UK), as described in the figure legends. For each GAG, injection of TGF-β1 pre-bound with a given dose of GAG was alternated with injection of TGF-β1 alone to ensure a stable baseline before obtaining readings for the following sample. Responses were measured as a function of time (sensogram) at 25°C. In competitive binding assays the maximum binding response for each condition was normalised to the response obtained from TGF-β1 alone. Competitive binding assays were repeated at least twice.

Downloaded from http://glycob.oxfordjournals.org/ at UniversitÃ¤tsbibliothek OsnabrÃ¼ck on January 12, 2016

Glycosaminoglycan (GAG) ELISA

To determine the ability of TGF-β1 to bind to GAG, positively-charged GAG-binding plates (Iduron, Manchester, UK) were utilised as a capture substrate. GAGs were passively adsorbed in each well and then challenged with TGF-β1 as previously described (Murali, et al. 2013). Briefly, wells were first pre-coated with 5 μg/mL of fully sulphated heparin or selectively desulphated heparin (Iduron, Manchester, UK). TGF-β1 was then added to the heparin-coated wells at a concentration of 100, 200, or 400 ng/mL and detection performed with mouse monoclonal anti-TGF-β1 antibody (MAB2401, R&D Systems, MN, USA) (750 ng/mL in blocking solution), goat polyclonal anti-mouse biotinylated antibody (ab6788, Abcam, Cambridge, UK) (1 μg/mL in blocking solution) and ExtrAvidin AP (Sigma-Aldrich) (220 ng/mL in blocking solution). Finally, development reagent (SigmaFAST p-Nitrophenyl phosphate, Sigma-Aldrich) was added, incubated at 37°C for 40 min and read at 405 nm.

Structural proteomics - "Protect and label" technique

The heparin-binding sites on TGF-β1 were identified by the "Protect and Label" approach, as described by Ori et al. (2009) for FGF-2, except that 1 nmol of TGF-β1 protein was employed and 0.1% (w/v) RapiGest^{TM} SF Surfactant (Waters Corporation, MA, USA) was used to elute the protein from the mini-column, because 2M NaCl proved inadequate. Digested and biotinylated peptides were purified on a C18 ZipTip (Merck Millipore, MA, USA) and then analysed by MS/MS. Up to 2 μg of the biotinylated peptides were injected into an LTQ Velos instrument (Thermo Fisher Scientific, MA, USA) using an EASY-nLC (Proxeon, Thermo Fisher Scientific). Peptides were separated on a PicoFrit^{TM} column (HALO, C18, 90 Å, 2.7 μm, 75 μm (internal diameter) x 100 mm length) (New Objectives, MA, USA) using a 60 min linear gradient (2–40% (v/v) acetonitrile in 0.1% formic acid). Data acquisition was performed using a TOP-10 strategy where survey MS scans were acquired in the dual pressure linear ion trap; MS scans ranged from 310 to 1400 m/z, with an automatic gain control (AGC) target of 3×10^4 and a maximum injection time of 10 ms. The 31 most intense ions with an ion intensity above 1000 and a charge state excluding one were sequentially isolated to a maximum AGC target value of 4×10^4 for a maximal 100 ms and fragmented by Collision Induced Dissociation (CID) using a normalised collision energy of 30%. A dynamic exclusion list was applied using an exclusion list size of 500, one repeat count, repeat duration of 45 s, exclusion duration of 30 s as well as a mass width of 1.0 low and 1.5 high. Expiration was disabled.

Downloaded from http://glycob.oxfordjournals.org/ at UniversitÃ¤tsbibliothek OsnabrÃ¼ck on January 12, 2016

Data analysis was performed using Mascot search (version 2.3, Matrix Science) using the ipi.HUMAN.v3.86.decoy database (183,568 sequences) and applying the following parameters: digest, chymotrypsin (FWYL/P); maximum missed cleavages, 2; Fixed modifications, carbamidomethyl (Cys); possible modifications, acetyl (Lys), acetyl (Protein N-term), biotin (Lys), oxidation (Met); parental ion tolerance, 2 Da; fragment ion tolerance, 0.8 Da. Biotinylated peptides with a Mascot score higher than 20 were manually validated.

Human MSC (hMSC) isolation, characterisation and cell culture

Primary hMSCs were isolated from commercially available bone marrow mononuclear cells (Lonza, MD, USA) of a young healthy adult human donor by plastic adherence and characterised as previously described (Rider, et al. 2008, Samsonraj, et al. 2013). Medium replacement was every three days. All experiments were carried out with cells at either passage 4 or 5.

Cell lysis and Western blotting

Human MSCs were cultured in 6-well plates in basal medium for 24 h at a density of 10,000 cells/cm^2. TGF-β1 treatments were then prepared at either 1 ng/mL or 5 ng/mL alone or in the presence of either 10 μg/mL or 40 μg/mL of full length heparin, or 1 ng/mL of TGF-β1 with 10 μg/mL size-fractionated or selectively desulphated heparin, and incubated at room temperature for 10 min before being added to the cells. The cells were then subjected to the various TGF-β1 treatments for 6, 12, 24 or 48 h and lysed in 2x Laemmli buffer (Sigma-Aldrich), before being resolved on a 4-12% (w/v gradient) SDS-PAGE gel. Samples were then immunoblotted with antibodies against SMAD2/3 (#3102, Cell Signaling, MA, USA), phosphorylated SMAD2 (pSMAD2) (#3108, Cell Signaling), phosphorylated SMAD3 (pSMAD3) (#9520, Cell Signaling) and actin (MAB1501R, Millipore). Densitometry was carried out using Quantity One and Image Studio Lite.

Heparinase treatment of hMSCs

Human MSCs were seeded in 8-well chamber slides at a density of 3,500 cells/cm^2 in basal medium. Cells were allowed to attach overnight before being treated with a combination of heparinase I, II and III (1.2 mIU/mL each), added directly to each well, for 24 h. To ensure that heparinase treatment effectively removed endogenous HS chains, remaining cell surface HS was detected by immunofluorescence using the 10E4 anti-HS antibody, which binds to intact HS (David, et al. 1992). Heparinase-treated cells were then fixed in 4% (w/v) paraformaldehyde in PBS for 10 min at room temperature, blocked with 3% (w/v)

Downloaded from http://glycob.oxfordjournals.org/ at UniversitÃ¤tsbibliothek OsnabrÃ¼ck on January 12, 2016

bovine serum albumin (BSA) in PBS for 30 min at room temperature and then incubated with the anti-HS 10E4 antibody (1:25 dilution in 0.3% (w/v) BSA-PBS) (AMS Biotechnology, Abingdon, UK) for 3 h at room temperature. Cells were then incubated with an anti-mouse IgM-FITC antibody (1:500 dilution in 0.3% (w/v) BSA-PBS) (BD Pharmingen^{TM}, Becton, Dickinson and Company, NJ, USA) for 45 min at room temperature and the nuclei stained with Hoechst 33342 (2 μg/mL in PBS) (Life Technologies) for 10 min at room temperature. Samples were imaged on an Olympus IX-81.

Cell signalling in heparinase-treated hMSCs

To assess the influence of endogenous HS on TGF-β1 signalling, Western blotting for pSMAD levels was performed on heparinase-treated hMSCs seeded at a density of 7,500 cells/cm^2 in 12-well plates in basal medium that were allowed to attach overnight. Medium was then changed to treatment medium (basal medium without serum that contained TGF-β1 (1 ng/mL or 5 ng/mL) alone or pre-incubated (10 min at room temperature) with heparin (10 μg/mL or 40 μg/mL)) for 6 h. Cells were then lysed for immunoblotting as previously described.

Statistical analysis

All results were analysed using two-tailed unpaired Student's *t*-test assuming unequal variances or one-way ANOVA using GraphPad Prism version 5.03; *P* values <0.05 were considered significant. Significant differences between treatment and relevant control levels are marked with a single (*) ($P < 0.05$), double (**) ($P < 0.01$), or triple (***) ($P < 0.001$) asterisk. Significant differences between treatments are indicated on the graphs.

Downloaded from http://glycob.oxfordjournals.org/ at UniversitÃ¤tsbibliothek OsnabrÃ¼ck on January 12, 2016

References

Baird A, Schubert D, Ling N, Guillemin R. 1988. Receptor- and heparin-binding domains of basic fibroblast growth factor. *Proceedings of the National Academy of Sciences*, 85:2324-2328.

Bramono DS, Murali S, Rai B, Ling L, Poh WT, Lim ZX, Stein GS, Nurcombe V, van Wijnen AJ, Cool SM. 2012. Bone marrow-derived heparan sulfate potentiates the osteogenic activity of bone morphogenetic protein-2 (BMP-2). *Bone*, 50:954-964.

Cardin AD, Weintraub HJ. 1989. Molecular modeling of protein-glycosaminoglycan interactions. *Arterioscler. Thromb. Vasc. Biol.*, 9:21-32.

David G, Bai XM, Van der Schueren B, Cassiman JJ, Van den Berghe H. 1992. Developmental changes in heparan sulfate expression: in situ detection with mAbs. *The Journal of Cell Biology*, 119:961-975.

Delehedde M, Lyon M, Gallagher JT, Rudland PS, Fernig DG. 2002. Fibroblast growth factor-2 binds to small heparin-derived oligosaccharides and stimulates a sustained phosphorylation of p42/44 mitogen-activated protein kinase and proliferation of rat mammary fibroblasts. . *Biochem. J.*, 366:235-244.

Duchesne L, Octeau V, Bearon RN, Beckett A, Prior IA, Lounis B, Fernig DG. 2012. Transport of Fibroblast Growth Factor 2 in the Pericellular Matrix Is Controlled by the Spatial Distribution of Its Binding Sites in Heparan Sulfate. *PLoS Biol.*, 10:e1001361.

Fairbrother WJ, Champe MA, Christinger HW, Keyt BA, Starovasnik MA. 1998. Solution structure of the heparin-binding domain of vascular endothelial growth factor. *Structure*, 6:637-648.

Fromm JR, Hileman RE, Caldwell EEO, Weiler JM, Linhardt RJ. 1995. Differences in the Interaction of Heparin with Arginine and Lysine and the Importance of these Basic Amino Acids in the Binding of Heparin to Acidic Fibroblast Growth Factor. *Arch. Biochem. Biophys.*, 323:279-287.

Downloaded from http://glycob.oxfordjournals.org/ at UniversitÃ¤tsbibliothek OsnabrÃ¼ck on January 12, 2016

Gandhi NS, Mancera RL. 2012. Prediction of heparin binding sites in bone morphogenetic proteins (BMPs). *Biochimica et Biophysica Acta (BBA) - Proteins and Proteomics*, 1824:1374-1381.

Gandrille S, Aiach M, Lane DA, Vidaud D, Molho-Sabatier P, Caso R, de Moerloose P, Fiessinger JN, Clauser E. 1990. Important role of arginine 129 in heparin-binding site of antithrombin III. Identification of a novel mutation arginine 129 to glutamine. *J. Biol. Chem.*, 265:18997-19001.

Grimaud E, Heymann D, Rédini F. 2002. Recent advances in TGF-β effects on chondrocyte metabolism: Potential therapeutic roles of TGF-β in cartilage disorders. *Cytokine Growth Factor Rev.*, 13:241-257.

Hames BD. 1998. *Gel Electrophoresis of Proteins : A Practical Approach: A Practical Approach* OUP Oxford.

Hernaiz M, Liu J, Rosenberg RD, Linhardt RJ. 2000. Enzymatic Modification of Heparan Sulfate on a Biochip Promotes Its Interaction with Antithrombin III. *Biochem. Biophys. Res. Commun.*, 276:292-297.

Hinck AP, Archer SJ, Qian SW, Roberts AB, Sporn MB, Weatherbee JA, Tsang MLS, Lucas R, Zhang B-L, Wenker J, *et al.* 1996. Transforming Growth Factor β1: Three-Dimensional Structure in Solution and Comparison with the X-ray Structure of Transforming Growth Factor β2. *Biochemistry*, 35:8517-8534.

Jakowlew S. 2006. Transforming growth factor-β in cancer and metastasis. *Cancer Metastasis Rev.*, 25:435-457.

Khan S, Gor J, Mulloy B, Perkins SJ. 2010. Semi-Rigid Solution Structures of Heparin by Constrained X-ray Scattering Modelling: New Insight into Heparin–Protein Complexes. *J. Mol. Biol.*, 395:504-521.

Lee J-H, Lee H, Joung YK, Jung KH, Choi J-H, Lee D-H, Park KD, Hong S-S. 2011. The use of low molecular weight heparin-pluronic nanogels to impede liver fibrosis by inhibition the TGF-β/Smad signaling pathway. *Biomaterials*, 32:1438-1445.

Downloaded from http://glycob.oxfordjournals.org/ at UniversitÃ¤tsbibliothek OsnabrÃ¼ck on January 12, 2016

Lee MJ. 2013. Heparin Inhibits Activation of Latent Transforming Growth Factor-β1. *Pharmacology*, 92:238-244.

Lin H, Lal R, Clegg DO. 2000. Imaging and Mapping Heparin-Binding Sites on Single Fibronectin Molecules with Atomic Force Microscopy†. *Biochemistry*, 39:3192-3196.

Lortat-Jacob H, Grosdidier A, Imberty A. 2002. Structural diversity of heparan sulfate binding domains in chemokines. *Proc. Natl. Acad. Sci. U. S. A.*, 99:1229-1234.

Lyon M, Rushton G, Gallagher JT. 1997. The Interaction of the Transforming Growth Factor-βs with Heparin/Heparan Sulfate Is Isoform-specific. *J. Biol. Chem.*, 272:18000-18006.

Manton KJ, Sadasivam M, Cool SM, Nurcombe V. 2006. Bone-specific heparan sulfates induce osteoblast growth arrest and downregulation of retinoblastoma protein. *J. Cell. Physiol.*, 209:219-229.

McCaffrey TA, Falcone DJ, Brayton CF, Agarwal LA, Welt FG, Weksler BB. 1989. Transforming growth factor-beta activity is potentiated by heparin via dissociation of the transforming growth factor-beta/alpha 2-macroglobulin inactive complex. *J. Cell Biol.*, 109:441-448.

McCaffrey TA, Falcone DJ, Du B. 1992. Transforming growth factor-β1 is a heparin-binding protein: Identification of putative heparin-binding regions and isolation of heparins with varying affinity for TGF-β1. *J. Cell. Physiol.*, 152:430-440.

McCaffrey TA, Falcone DJ, Vicente D, Du B, Consigli S, Borth W. 1994. Protection of transforming growth factor β activity by heparin and fucoidan. *J. Cell. Physiol.*, 159:51-59.

Mu E, Ding R, An X, Li X, Chen S, Ma X. 2012. Heparin attenuates lipopolysaccharide-induced acute lung injury by inhibiting nitric oxide synthase and TGF-β/Smad signaling pathway. *Thromb. Res.*, 129:479-485.

Murali S, Leong DFM, Lee JJL, Cool SM, Nurcombe V. 2011. Comparative Assessment of the Effects of Gender-specific Heparan Sulfates on Mesenchymal Stem Cells. *J. Biol. Chem.*, 286:17755-17765.

Downloaded from http://glycob.oxfordjournals.org/ at UniversitÃ¤tsbibliothek OsnabrÃ¼ck on January 12, 2016

Murali S, Manton KJ, Tjong V, Su X, Haupt LM, Cool SM, Nurcombe V. 2009. Purification and characterization of heparan sulfate from human primary osteoblasts. *J. Cell. Biochem.*, 108:1132-1142.

Murali S, Rai B, Dombrowski C, Lee JLJ, Lim ZXH, Bramono DS, Ling L, Bell T, Hinkley S, Nathan SS, *et al.* 2013. Affinity-selected heparan sulfate for bone repair. *Biomaterials*, 34:5594-5605.

Murphy KJ, Merry CLR, Lyon M, Thompson JE, Roberts IS, Gallagher JT. 2004. A New Model for the Domain Structure of Heparan Sulfate Based on the Novel Specificity of K5 Lyase. *J. Biol. Chem.*, 279:27239-27245.

Nurcombe V, Goh F, Haupt L, Murali S, Cool S. 2007. Temporal and functional changes in glycosaminoglycan expression during osteogenesis. *J Mol Hist*, 38:469-481.

Ori A, Free P, Courty J, Wilkinson MC, Fernig DG. 2009. Identification of Heparin-binding Sites in Proteins by Selective Labeling. *Mol. Cell. Proteomics*, 8:2256-2265.

Ori A, Wilkinson MC, Fernig DG. 2008. The heparanome and regulation of cell function: structures, functions and challenges. *Front. Biosci.*, 13:4309-4338.

Ori A, Wilkinson MC, Fernig DG. 2011. A systems biology approach for the investigation of the heparin/heparan sulfate interactome. *J. Biol. Chem.*

Rider DA, Dombrowski C, Sawyer AA, Ng GHB, Leong D, Hutmacher DW, Nurcombe V, Cool SM. 2008. Autocrine Fibroblast Growth Factor 2 Increases the Multipotentiality of Human Adipose-Derived Mesenchymal Stem Cells. *Stem Cells*, 26:1598-1608.

Rosen F, McCabe G, Quach J, Solan J, Terkeltaub R, Seegmiller JE, Lotz M. 1997. Differential effects of aging on human chondrocyte responses to transforming growth factor beta. Increased pyrophosphate production and decreased cell proliferation. *Arthritis Rheum.*, 40:1275-1281.

Samsonraj RM, Raghunath M, Hui JH, Ling L, Nurcombe V, Cool SM. 2013. Telomere length analysis of human mesenchymal stem cells by quantitative PCR. *Gene*, 519:348-355.

San Antonio JD, Lander AD, Karnovsky MJ, Slayter HS. 1994. Mapping the heparin-binding sites on type I collagen monomers and fibrils. *The Journal of Cell Biology*, 125:1179-1188.

Downloaded from http://glycob.oxfordjournals.org/ at UniversitÃ¤tsbibliothek OsnabrÃ¼ck on January 12, 2016

Sato M, Ishihara M, Ishihara M, Kaneshiro N, Mitani G, Nagai T, Kutsuna T, Asazuma T, Kikuchi M, Mochida J. 2007. Effects of growth factors on heparin-carrying polystyrene-coated atelocollagen scaffold for articular cartilage tissue engineering. *J Biomed Mater Res B Appl Biomater*, 83B:181-188.

Shi M, Zhu J, Wang R, Chen X, Mi L, Walz T, Springer TA. 2011. Latent TGF-β structure and activation. *Nature*, 474:343-349.

Siebert N, Xu W, Grambow E, Zechner D, Vollmar B. 2011. Erythropoietin improves skin wound healing and activates the TGF-β signaling pathway. *Lab. Invest.*, 91:1753-1765.

Soker S, Goldstaub D, Svahn CM, Vlodavsky I, Levi BZ, Neufeld G. 1994. Variations in the Size and Sulfation of Heparin Modulate the Effect of Heparin on the Binding of VEGF165 to Its Receptors. *Biochem. Biophys. Res. Commun.*, 203:1339-1347.

Sweeney SM, Guy CA, Fields GB, Antonio JDS. 1998. Defining the domains of type I collagen involved in heparin- binding and endothelial tube formation. *Proceedings of the National Academy of Sciences*, 95:7275-7280.

Toh WS, Liu H, Heng BC, Rufaihah AJ, Ye CP, Cao T. 2005. Combined effects of TGFβ1 and BMP2 in serum-free chondrogenic differentiation of mesenchymal stem cells induced hyaline-like cartilage formation. *Growth Factors*, 23:313-321.

Uniewicz KA, Ori A, Ahmed YA, Yates EA, Fernig DG. 2014. Characterisation of the interaction of neuropilin-1 with heparin and a heparan sulfate mimetic library of heparin-derived sugars. *PeerJ*, 2:e461.

van der Kraan PM, Blaney Davidson EN, Blom A, van den Berg WB. 2009. TGF-beta signaling in chondrocyte terminal differentiation and osteoarthritis: Modulation and integration of signaling pathways through receptor-Smads. *Osteoarthritis Cartilage*, 17:1539-1545.

Vivès RR, Crublet E, Andrieu J-P, Gagnon J, Rousselle P, Lortat-Jacob H. 2004. A Novel Strategy for Defining Critical Amino Acid Residues Involved in Protein/Glycosaminoglycan Interactions. *J. Biol. Chem.*, 279:54327-54333.

Downloaded from http://glycob.oxfordjournals.org/ at UniversitÃ¤tsbibliothek OsnabrÃ¼ck on January 12, 2016

Wahl SM, Hunt DA, Wakefield LM, McCartney-Francis N, Wahl LM, Roberts AB, Sporn MB. 1987. Transforming growth factor type beta induces monocyte chemotaxis and growth factor production. *Proceedings of the National Academy of Sciences*, 84:5788-5792.

Wang W, Li B, Li Y, Jiang Y, Ouyang H, Gao C. 2010. In vivo restoration of full-thickness cartilage defects by poly(lactide-co-glycolide) sponges filled with fibrin gel, bone marrow mesenchymal stem cells and DNA complexes. *Biomaterials*, 31:5953-5965.

Wang W, Rigueur D, Lyons KM. 2014. TGFβ signaling in cartilage development and maintenance. *Birth Defects Research Part C: Embryo Today: Reviews*, 102:37-51.

Watson RS, Gouze E, Levings PP, Bush ML, Kay JD, Jorgensen MS, Dacanay EA, Reith JW, Wright TW, Ghivizzani SC. 2010. Gene delivery of TGF-β1 induces arthrofibrosis and chondrometaplasia of synovium in vivo. *Lab. Invest.*, 90:1615-1627.

Xu R, Ori A, Rudd TR, Uniewicz KA, Ahmed YA, Guimond SE, Skidmore MA, Siligardi G, Yates EA, Fernig DG. 2012. Diversification of the Structural Determinants of Fibroblast Growth Factor-Heparin Interactions: IMPLICATIONS FOR BINDING SPECIFICITY. *J. Biol. Chem.*, 287:40061-40073.

Yang X, Chen L, Xu X, Li C, Huang C, Deng C-X. 2001. TGF-β/Smad3 Signals Repress Chondrocyte Hypertrophic Differentiation and Are Required for Maintaining Articular Cartilage. *J. Cell Biol.*, 153:35-46.

Yang Y-a, Dukhanina O, Tang B, Mamura M, Letterio JJ, MacGregor J, Patel SC, Khozin S, Liu Z-y, Green J, *et al.* 2002. Lifetime exposure to a soluble TGF-β antagonist protects mice against metastasis without adverse side effects. *J. Clin. Invest.*, 109:1607-1615.

Yates EA, Santini F, Guerrini M, Naggi A, Torri G, Casu B. 1996. 1H and 13C NMR spectral assignments of the major sequences of twelve systematically modified heparin derivatives. *Carbohydr. Res.*, 294:15-27.

Yue X, Li X, Nguyen HT, Chin DR, Sullivan DE, Lasky JA. 2008. Transforming Growth Factor-β1 Induces Heparan Sulfate 6-O-Endosulfatase 1 Expression *in Vitro* and *in Vivo*. *J. Biol. Chem.*, 283:20397-20407.

Downloaded from http://glycob.oxfordjournals.org/ at UniversitÃ¤tsbibliothek OsnabrÃ¼ck on January 12, 2016

Abbreviations

dp	Degree of polymerisation
ECM	Extracellular matrix
ELISA	Enzyme-linked immunosorbent assay
FGF-2	Fibroblast growth factor-2
GAG	Glycosaminoglycan
GlcA	Glucuronic acid
hMSC	Human Mesenchymal stem cell
HS	Heparan sulphate
IdoA	Iduronic acid
LTGF	Latent transforming growth factor-β
MS/MS	Tandem mass spectrometry
NHS	*N*-hydroxysuccinimide
pSMAD2	Phospho-SMAD2
pSMAD3	Phospho-SMAD3
RU	Response unit
SAB	Standard assay buffer
TGF-β1	Transforming growth factor-β1

Downloaded from http://glycob.oxfordjournals.org/ at UniversitÃ¤tsbibliothek OsnabrÃ¼ck on January 12, 2016

Figure legends

FIGURE 1. Heparin binds to TGF-β1. **(A)** SPR sensogram showing the background subtracted change in binding response to various concentrations (50 to 800 nM) of injected TGF-β1 over a heparin-coated surface. Sensogram is representative of 2 independent experiments. **(B)** GAG ELISA to determine the ability of TGF-β1 to bind to heparin. Error bars represent standard deviation, n = 3.

FIGURE 2. The "Protect and Label" structure proteomics technique. **(A)** Schematic summarising the steps in the "Protect and Label" technique. Note that RapiGest was used to elute the "protected" protein instead of 2M NaCl. Figure adapted from Ori et al. (2009). **(B)** Silver stained gel showing the quality control samples of TGF-β1 taken at the indicated stages of the "Protect and Label" experiment. The TGF-β1 homodimer runs at 25 kDa while the monomer runs at 12.5 kDa. NHS – n-hydroxysuccinimide, MS – Mass spectrometry. Gel is representative of 2 independent experiments.

FIGURE 3. Identification of TGF-β1 heparin-binding sites. **(A)** The TGF-β1 amino acid sequence and position of lysines identified by the "Protect and label" strategy. The previously published predicted heparin-binding domain (HBD) of TGF-β1 is underlined. Lysines we identified with high confidence (*) and medium confidence (^) are indicated. **(B)** The positions of the identified lysines mapped onto the 3-dimensional structure of TGF-β1 (PDB: 1KLC (Hinck, et al. 1996)). The newly identified lysines are coloured blue and those overlapping with the literature-annotated heparin-binding sites are coloured green. Top row, ribbon diagram. Bottom row, corresponding molecular surface. Residues are only labelled on one of the TGF-β1 monomers. The figures were prepared using PyMOL.

FIGURE 4. Biacore competition assays to determine heparin length requirements for TGF-β1 binding. Representative SPR sensograms showing the changes in binding response of 200 nM of TGF-β1 when pre-incubated with either 5 or 10 μg of **(A)** dp4, **(B)** dp12, **(C)** dp20 or **(D)** heparin (Hep) prior to injection. **(E)** Bar chart depicts the ability of the various GAGs to compete for TGF-β1 binding against the heparin-coated surface. For clarity, the binding response of TGF-β1 without any GAG (i.e. 0 μg) is only shown for heparin. Data were normalised to 200 nM TGF-β1 alone. Error bars represent standard deviation, *n* = 3.

Downloaded from http://glycob.oxfordjournals.org/ at UniversitÃ¤tsbibliothek OsnabrÃ¼ck on January 12, 2016

FIGURE 5. Biacore competition assays to determine heparin sulphation requirements for TGF-β1 binding. Representative SPR sensograms showing the changes in binding response of 200 nM of TGF-β1 when pre-incubated with either 5 or 10 μg of **(A)** 2-*O*-desulphated heparin (2-*O*-de), **(B)** 6-*O*-desulphated heparin (6-*O*-de), **(C)** *N*-desulphated re-*N*-acetylated heparin (*N*-de) or **(D)** heparin (Hep) prior to injection. **(E)** Representative bar chart depicts the ability of the various GAGs **(A-D)** to compete for TGF-β1 binding against the heparin-coated surface. For clarity, the binding response of TGF-β1 without any GAG (i.e. 0 μg) is only shown for heparin. Data were normalised to 200 nM TGF-β1 alone. Results are representative of 2 independent experiments.

FIGURE 6. Optimisation of TGF-β1 dosing in hMSCS. Passage 5 cells were treated with various doses of TGF-β1 and lysed at the indicated time points. Phosphorylated SMAD2 (pSMAD2), phosphorylated SMAD3 (pSMAD3), total SMAD2/3 (SMAD2/3) and actin levels were detected by Western blotting. Blots are representative of 3 independent experiments.

FIGURE 7. Effect of heparin on TGF-β1 signalling in hMSCs. Passage 5 cells were treated with the indicated doses of TGF-β1 that had been pre-incubated with either 10 or 40 μg/ml of heparin and lysed after 6 h. Phosphorylated SMAD2 (pSMAD2), phosphorylated SMAD3 (pSMAD3), total SMAD2/3 (SMAD2/3) and actin levels were detected by Western blotting. Blots are representative of 3 independent experiments.

FIGURE 8. Heparinase treatment does not affect TGF-β1 signalling in hMSCs. Cell surface HS expression after 24 h **(A)** without (- Heparinase) or **(B)** with heparinase (+ Heparinase) treatment. HS was stained with 10E4 antibody (green, FITC-conjugate secondary antibody) and nuclei were stained with Hoechst 33342 (blue). Western blot analysis of passage 5 hMSCs treated **(C)** without (- Heparinase) or **(D)** with heparinase (+ Heparinase) for 24 h prior to treatment (6 h) with the indicated doses of TGF-β1 and/or heparin (Hep). Scale bar: 50 μm. Data is compiled from a single experiment.

FIGURE 9. Effect of heparin **(A)** length and **(B)** sulphation on TGF-β1 signalling in hMSCs. Cells were treated with TGF-β1 (1 ng/ml), pre-incubated with 10 μg/ml of the various heparin fragments (dp14-24), selectively desulphated heparins (2-*O*-de, 6-*O*-de and *N*-de) or heparin (Hep) for 10 min at room temperature, and lysed at 6 h. Phosphorylated SMAD2

Downloaded from http://glycob.oxfordjournals.org/ at UniversitÃ¤tsbibliothek OsnabrÃ¼ck on January 12, 2016

(pSMAD2) and SMAD3 (pSMAD3), total SMAD2/3 and actin levels were determined by Western blotting. Blots are representative of 3 independent experiments.

FIGURE 10. Proposed model for heparin-TGF-β1 binding. According to the model proposed by Lyon et al. (1997) (image adapted from Lyon et al. 1997) **(A)**, the heparin/HS chain (red and orange chain representing a dp26 fragment) interacts with TGF-β1 through the K304 (K26 on the Lyon *et al.* model) residue on either monomer **(B)**. This model would involve the heparin/HS chain (red and orange chain representing the alternating uronic acid and glucosamine residues) having to navigate the groove between the interfaces of the two protein monomers. The position of K291 (dark blue identified by Protect and Label) would aid the GAG chain in the adoption of such a spatial orientation needed for binding to TGF-β1. Comparison of the predicted TGF-β1 structure with recently published heparin structures by Khan et al. (2010) also suggests that a dp22 heparin fragment would be sufficient to bridge the distance between the K304 residues on either monomer. **(C)** Ribbon diagram of porcine LTGF-β1 demonstrating how the latency associate peptide (LAP) (beige) wraps around the TGF-β1 homodimer (grey) (PDB: 3RJR (Shi, et al. 2011)). Applying the same heparin-binding model from Figure 10B to the LTGF-β1 structure, the K291 residues may aid in the orientation of the heparin/HS chain (red and orange chain) to interfere with the binding of LAP (beige) to mature TGF-β1 **(D)**. Alternatively, the arrangement of the basic residues in the arms of LAP may serve to bind heparin/HS in a way that stabilises the LTGF-β1 complex (Lee 2013) **(E)**. Basic residues in LTGF-β1 are coloured light blue.

Downloaded from http://glycob.oxfordjournals.org/ at UniversitÃ¤tsbibliothek OsnabrÃ¼ck on January 12, 2016

Tables

TABLE 1. Summary of peptides identified by "Protect and Label" structure proteomics. Labelled peptides were identified by tandem mass spectrometry and analysed by Mascot search Version 2.4 (Matrix Science). Here, a summary of the peptides involved in the heparin-binding sites and the labelled position is provided. A full list of identified peptides is provided in the supplementary materials (Table S1).

Peptide	Ion(s)[a]	Sequence	Residues[b]
1	23,24,25,26, 27,28	C(carbamidomethyl)FSSTEK(biotin)NC(carbamidomethyl)C(carbamidomethyl)VRQLY	285-299
2	22	SSTEK(acetyl)NC(carbamidomethyl)C(carbamidomethyl)VRQLY	287-299
3	1,3,7	IDFRK(biotin)DLGW	300-308
4	1,5,12	RK(biotin)DLGWK(acetyl)W	303-310
5	4,6,21	RK(acetyl)DLGWK(biotin)W	303-310
6	2,12,13,21	IHEPK(biotin)GY	311-317
7	8	SLDTQYSK(biotin)VL	331-340
8	10,16,20, 29,31	YVGRK(biotin)PK(acetyl)VEQL	369-379
9	10,11,18, 19,20,29,30	YVGRK(acetyl)PK(biotin)VEQL	369-379
10	14,15,17	SNMIVRSC(carbamidomethyl)K(biotin)C(carbamidomethyl)S	380-390
11	9,30,31	SNMIVRSC(carbamidomethyl)K(acetyl)C(carbamidomethyl)S	380-390

[a] Ions numbered according to Table S1

[b] Residues numbered according to Fig. 3.

Downloaded from http://glycob.oxfordjournals.org/ at UniversitÃ¤tsbibliothek OsnabrÃ¼ck on January 12, 2016

Downloaded from http://glycob.oxfordjournals.org/ at UniversitÃ¤tsbibliothek OsnabrÃ¼ck on January 12, 2016

Figure 1

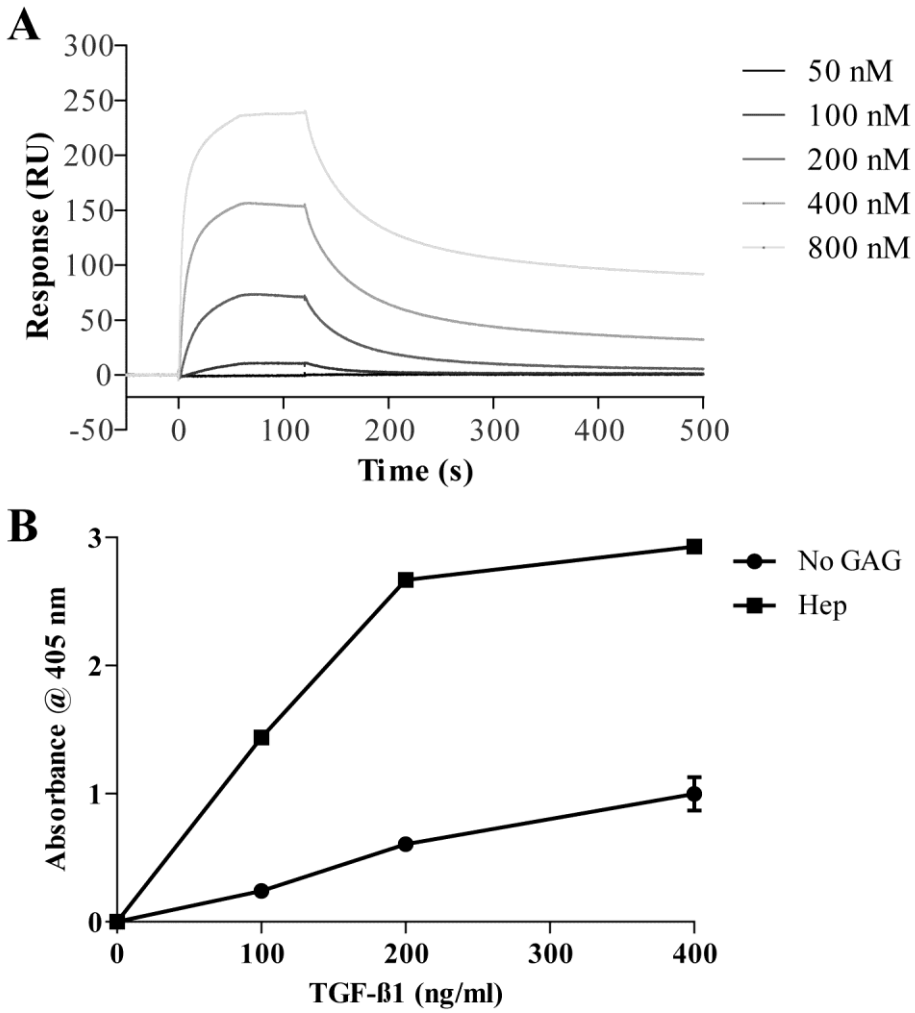

Downloaded from http://glycob.oxfordjournals.org/ at UniversitÃ¤tsbibliothek Osnabrück on January 12, 2016

Figure 2

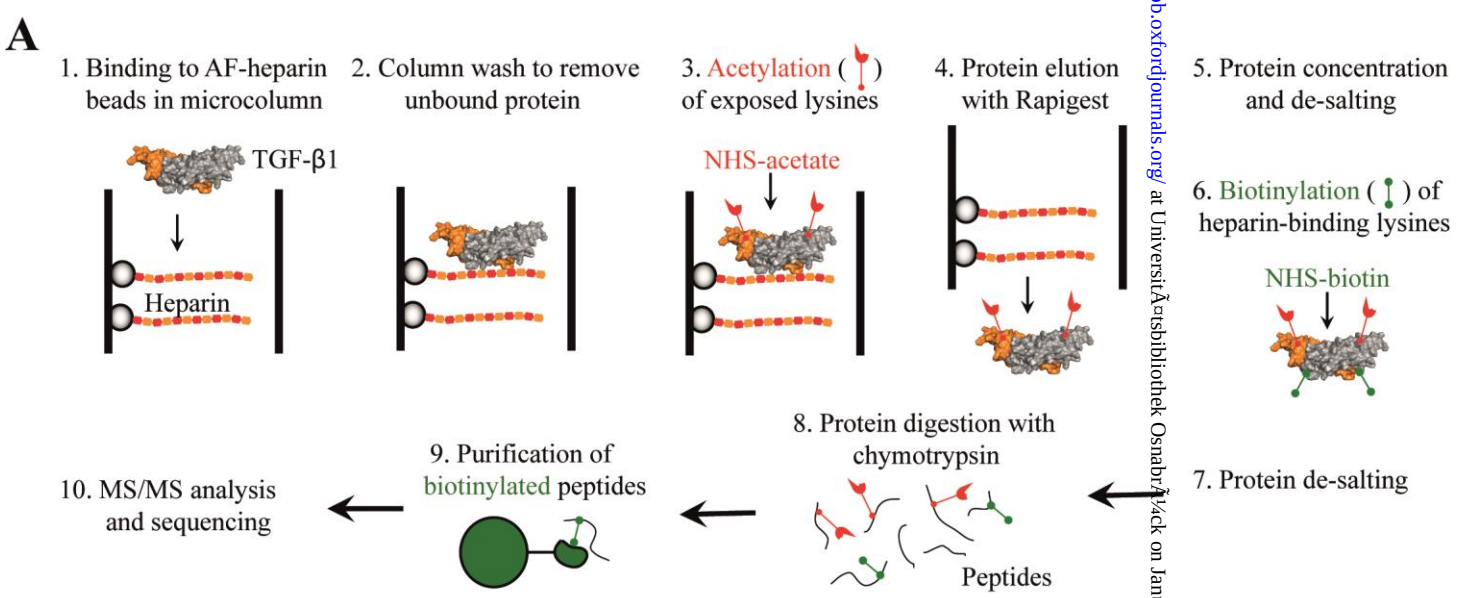

B

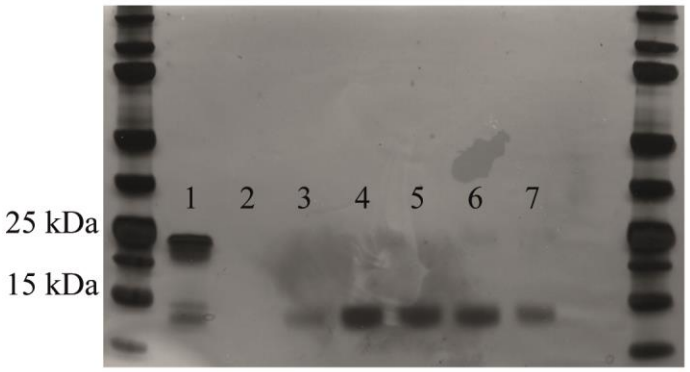

Sample No	Sample contents
1	Original protein sample
2	1st wash after loading
3	Flow through after acetylation
4	Eluted protein
5	Concentrated & de-salted protein
6	Biotinylated protein
7	De-salted protein

Downloaded from http://glycob.oxfordjournals.org/ at UniversitÃ¤tsbibliothek Osnabrück on January 12, 2016

Figure 3

A

```
          280        290        300        310        320        330
           AL DTNYCFSSTE *KNCCVRQLYI DFR*DLGW*KW IHEP*GYHAN FCLGPCPYIW

          340        350        360        370        380        390
SLDTQYS^KVL ALYNQHNPGA SAAPCCVPQA LEPLPIVYYV GR*KP*KVEQLS NMIVRS*KCS
```

Published predicted HBD
*Lysines identified with high confidence
^Lysines identified with medium confidence

B

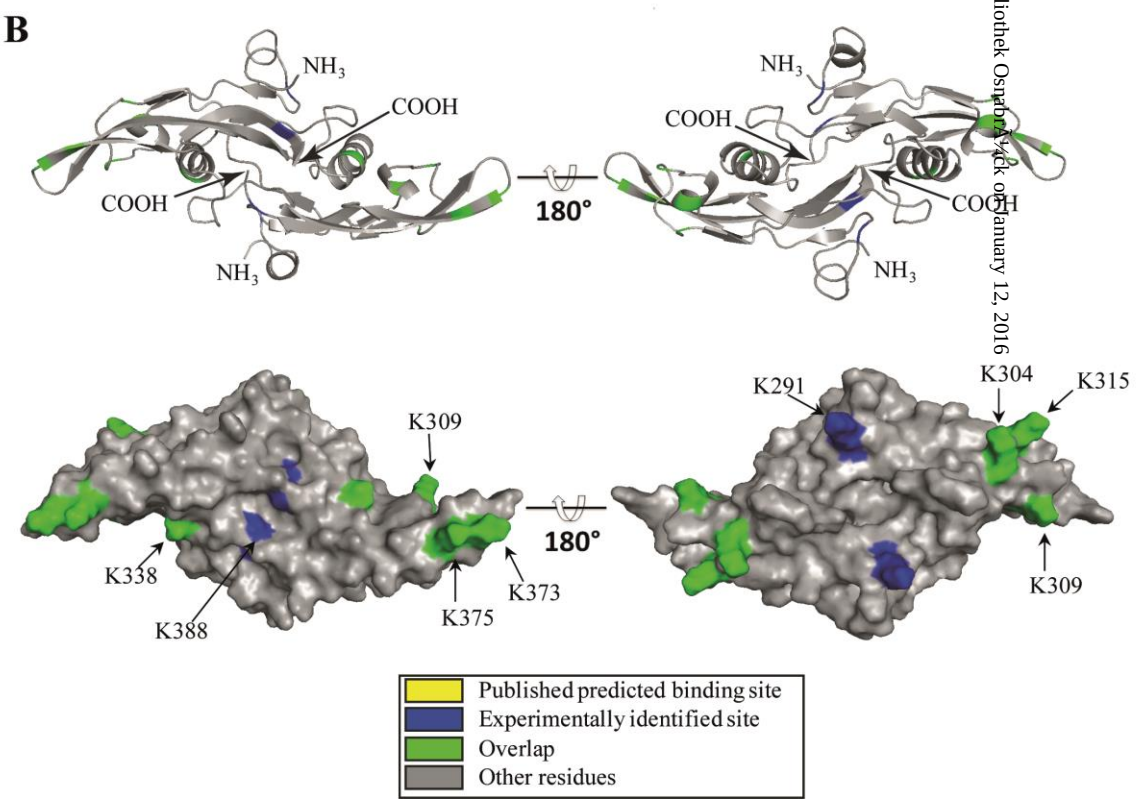

Downloaded from http://glycob.oxfordjournals.org/ at UniversitÃ¤tsbibliothek OsnabrÃ¼ck on January 12, 2016

Figure 4

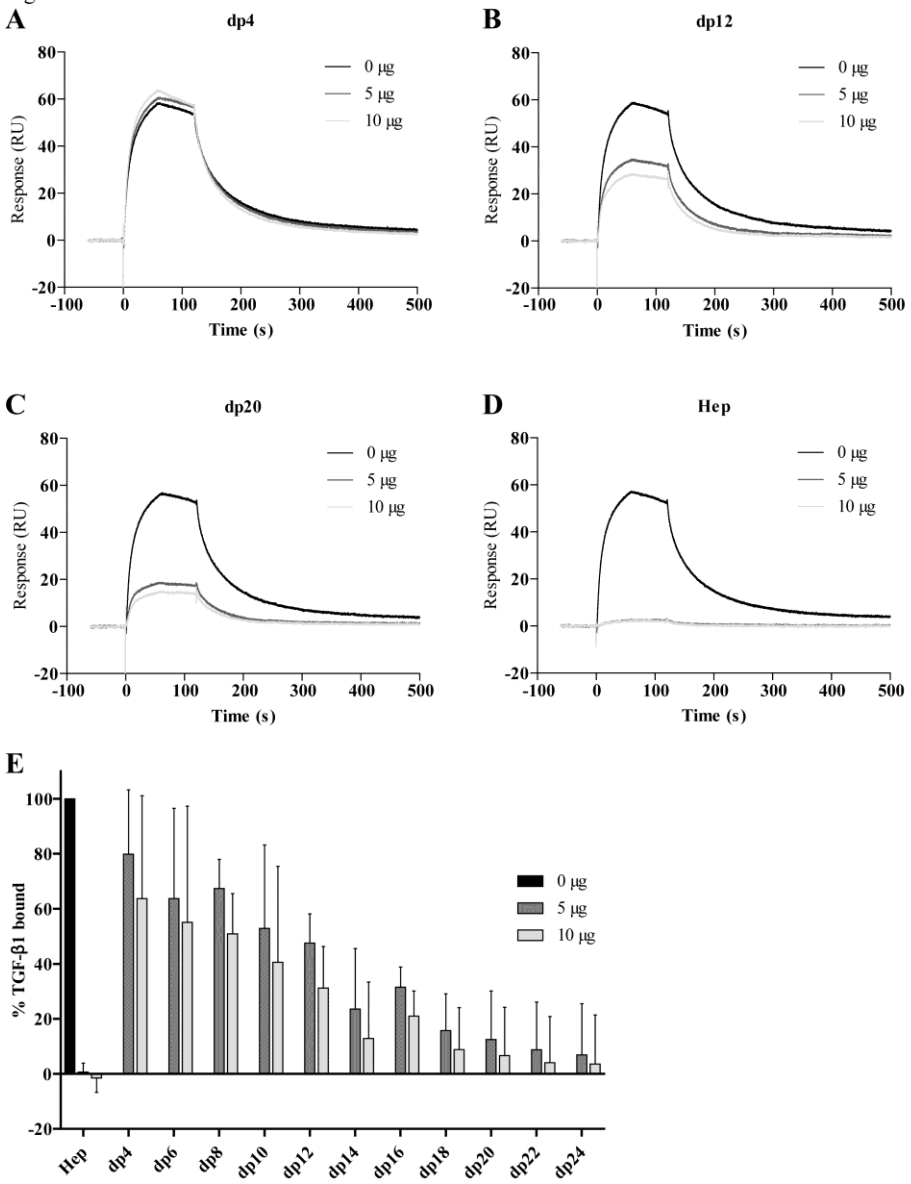

Figure 5

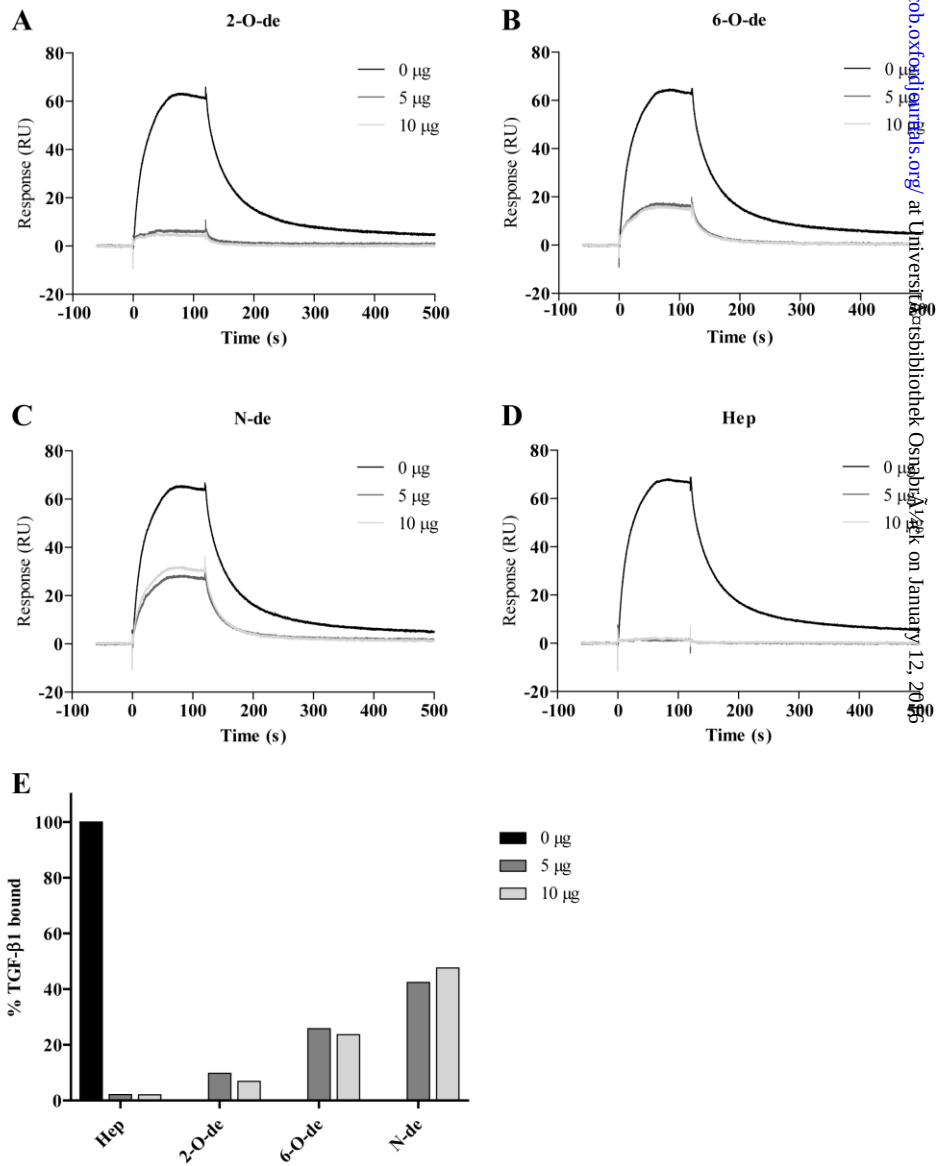

Downloaded from http://glycob.oxfordjournals.org/ at Universitaetsbibliothek Osnabrueck on January 12, 2015

Figure 6

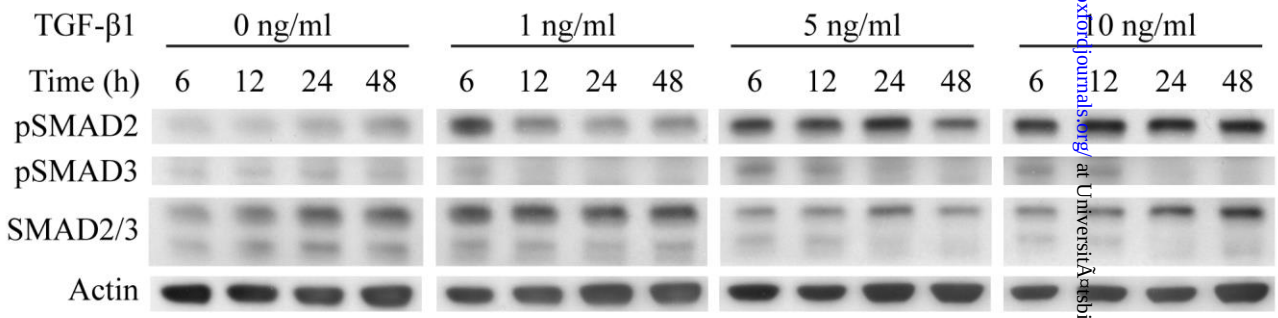

Downloaded from http://glycob.oxfordjournals.org/ at UniversitÃ¤tsbibliothek OsnabrÃ¼ck on January 12, 2016

Figure 7

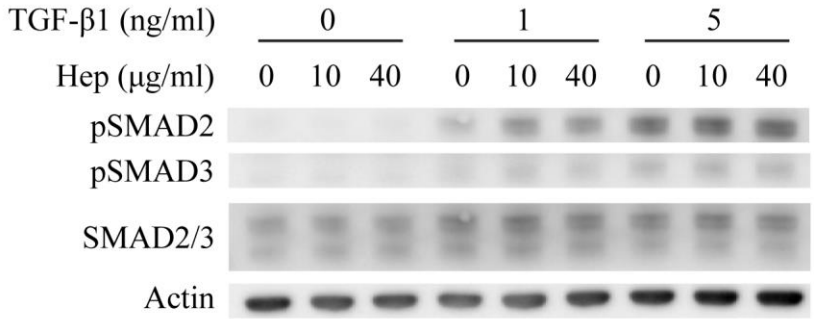

Downloaded from http://glycob.oxfordjournals.org/ at UniversitÃ¤tsbibliothek OsnabrÃ¼ck on January 12, 2016

Downloaded from http://glycob.oxfordjournals.org/ at University of Toronto Libraries on January 12, 2016

Figure 8

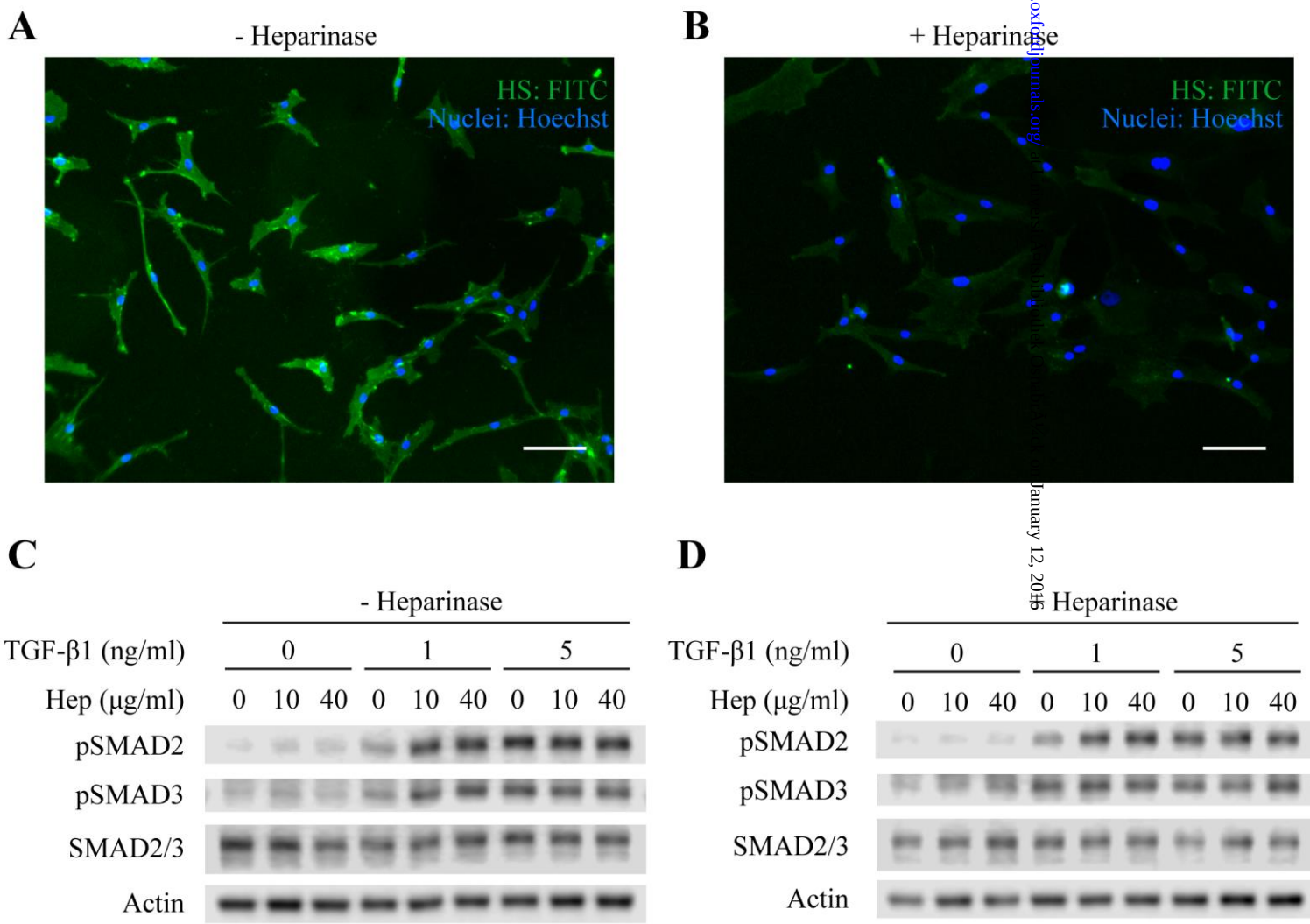

Downloaded from http://glycob.oxfordjournals.org/ at UniversitÃ¤tsbibliothek OsnabrÃ¼ck on January 12, 2016

Figure 9

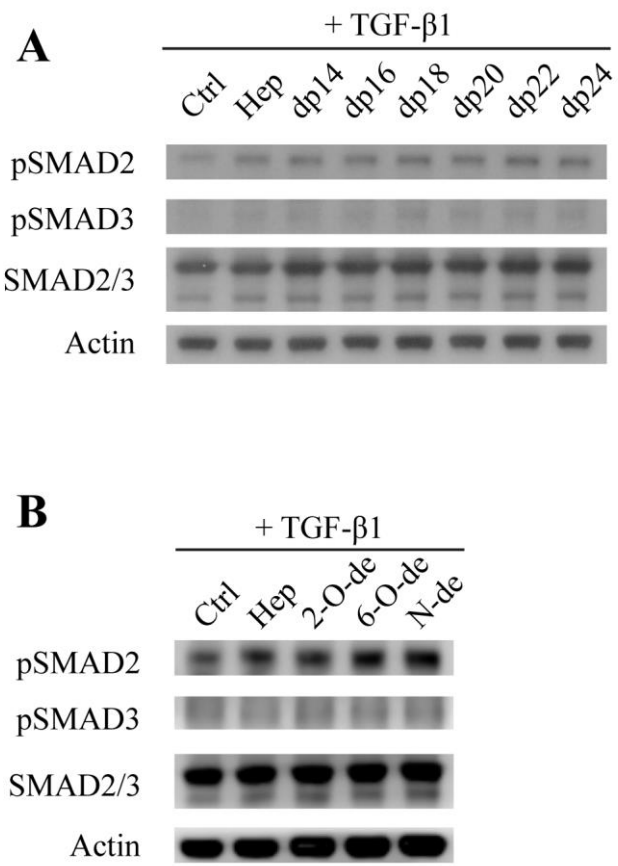

Downloaded from http://glycob.oxfordjournals.org/ at Universitätsbibliothek Osnabrück on January 12, 2016

Figure 10